16th World Congress in Computational Mechanics (WCCM)
21-26 July 2024, Vancouver, Canada
J. H. Guan, X. Zhou, G. H. Qu and G. Bao (Eds)

ENHANCED MECHANICAL BEHAVIOR OF NICKEL-COATED GRAPHENE GRAPHENE REINFORCED COCRFEMNNI NANOLAYERED COMPOSITES

JUNHAO GUAN [1], XIA ZHOU [1], GUOHUI QU [2] AND GEORGE BAO [3]

[1]Dalian University of Technology
No. 2 Ling Gong Road, Ganjingzi District, Dalian City, Liaoning Province, 116024, China
3040466650@qq.com

[1]Dalian University of Technology
No. 2 Ling Gong Road, Ganjingzi District, Dalian City, Liaoning Province, 116024, China
zhouxia@dlut.edu.cn, http://faculty.dlut.edu.cn/zhouxia/zh_CN/index.htm

[2]Dalian Xinzhong Group Co., LTD.
Beihai Economic Developing Zone Dalian Bay Town, Dalian 116113, China
quguohui@xinzhonggroup.cn, http://www.xinzhonggroup.cn

[3]Peninsula Alloy Inc, Stevensville
Research and Development Division, Peninsula Alloy Inc, Stevensville, Canada
baozhiyong@gmail.com

Key words: HEAs, Nickel-Coated Graphene, Strengthening Effect, MD Simulation.

Abstract. High entropy alloys (HEAs) especially CoCrFeMnNi HEAs have drawn more and more attention due to their excellent combination performance. However, the mechanical properties of CoCrFeMnNi HEAs still remain to be improved due to the single-phase FCC crystal structure. Although many efforts have been made on strengthening methods by grain refinement or nitriding the improvement of the mechanical properties is still unsatisfactory. To improve the mechanical properties of CoCrFeMnNi HEAs and broaden their application fields, we proposed that adding functionalized graphene in CoCrFeMnNi HEAs and investigated nanoscale mechanical properties and the strengthening mechanism using molecular dynamics (MD) simulation in this paper. The mechanical properties of pristine single-layer graphene nanoplatelets (GNPs) and double-side nickel-coated GNP (Ni-GNP-Ni) reinforced CoCrFeMnNi composites (Ni-GNP-Ni/CoCrFeMnNi) are studied under uniaxial tension by molecular dynamics (MD) simulations. The simulated results show that the mechanical properties of Ni-GNP-Ni/CoCrFeMnNi composites are improved significantly by the addition of Ni coated GNPs. The mechanical properties of Ni-GNP-Ni/CoCrFeMnNi composites exhibit temperature softening and strain rate strengthening effect, and their tensile mechanical properties such as the tensile strength, fracture strain decrease with increasing temperature and enhance with increasing strain rate. It is concluded that the main strengthening mechanisms for Ni-GNP-Ni/CoCrFeMnNi composites are strong interface bonding, effective load transfer from the CoCrFeMnNi matrix to the Ni-GNP-Ni and dislocation/twin strengthening by analysis of the evolution of atomic structure.

1 INTRODUCTION

The multicomponent high-entropy alloys (HEAs) are promising candidate materials in aviation aerospace, military and nuclear applications due to their unique design concept different from traditional alloys and excellent mechanical properties. Among various HEA systems, the face-centered cubic (FCC) structure CoCrFeMnNi HEA with a single-phase has been widely investigated due to its exceptional strength and fracture toughness at cryogenic temperature, but the lower room temperature strength is limited for structural applications [1]. To further improve the yield strength of FCC CoCrFeMnNi HEAs, considerable efforts have been made to explore the strengthening strategies including gradient grain refinement [2] or metal doping regulation [3,4] and non-metallic atoms doping such as C, B and N [5,6], but the development of novel CoCrFeMnNi HEA matrix composites with a superior combination of high strength and good ductility is still an outstanding issue.

An effective method towards enhanced properties is to incorporate a nanosized reinforcing phase into the HEA matrix, obtaining laminated HEA matrix composites [7], while the interface has a significant impact on the mechanical properties of nanolaminated composite materials. Graphene and its various derivatives have been widely used as reinforcing phase in metal matrix [8] due to their high strength, great toughness, and the ability to improve interfacial load transfer. The graphene reinforced HEA matrix composites have been successfully fabricated [7,9,10] recently. Premlata et al. [9] investigated the Graphene oxide (GO) reinforced CuNiFeCrMo HEA nano composite coating and found that the composite coating showed enhanced mechanical and surface properties. Liu et al. [7,10] introduced Ni plated graphene films (GFs) to the CoCrFeNiMn high-entropy alloy (HEA) matrix based on their early study and prepared the GFs(Ni)/HEA matrix laminated composites. As a result, the strength and ductility of the CoCrFeNiMn alloy were both improved. Despite some progress has been made in improving mechanical properties of the graphene reinforced high entropy alloy composites, the underlying strengthening and deformation mechanisms of graphene-reinforced HEA composites at the nanoscale are still poorly understood.

In the present paper, MD simulation was conducted to investigate the tensile properties and strengthening mechanism of Ni-coated graphene nanoplatelets (GNPs) reinforced CoCrFeMnNi HEA laminated composites under uniaxial tension by considering the coupled effects of temperature and strain rate. It is expected that the research result would provide a valuable reference for the structural design and property enhancement of graphene reinforced CoCrFeMnNi HEA matrix composites.

2 SIMULATION MODEL AND METHOD

2.1 Model establishmen

Fig. 1 shows the atomic model of single-phase FCC CoCrFeMnNi HEA matrix composites reinforced by monolayer graphene coated with double sides Nickel (Ni-GNP-Ni) for MD simulation. The *x*, *y*, and *z* axes were consistent to the [$0\bar{1}1$], [100] and [011] crystallographic

directions of HEA-matrix, respectively. For the CoCrFeMnNi HEA matrix with the lattice constant of 3.593 Å, it has the size of 8.5 nm × 9.8 nm × 8.5 nm and contains 63920 atoms. For the Ni-GNP-Ni sheet, the thickness of monolayer GNP itself was 0.34 nm, while the distance between Ni and C atoms on the surface of GNP was 0.15nm. The atomic configurations for the composites were established by first constructing the Ni single crystal and then randomly replacing Ni atoms with other four atoms (Co, Cr, Fe and Mn) in identical proportion and subsequently inserting Ni-GNP-Ni sheet into the matrix along the *x*-*y* plane in which the zigzag and armchair edges in Ni-GNP-Ni are separately parallel to the *x*-axis and *y*-axis. In addition, the HEA-matrix atoms that within a distance of 2.5 Å from the Ni-GNP-Ni sheet were removed to avoid atom overlapping.

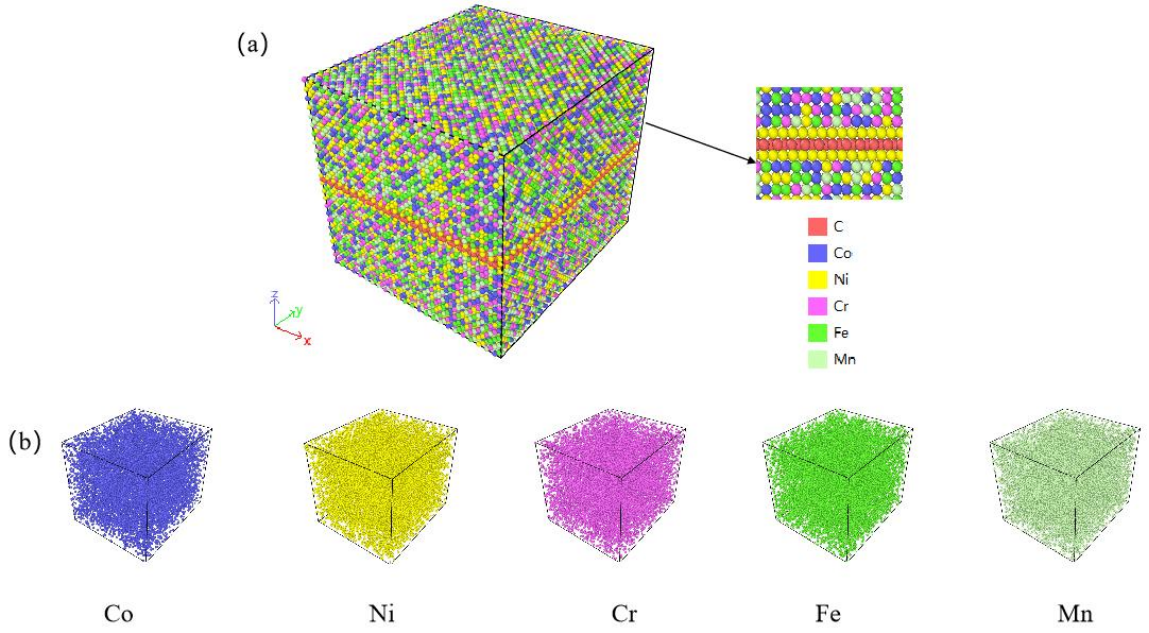

Figure 1: (a) Atomistic models of Ni-Gr-Ni/CoCrFeMnNi laminated composites; (b) atomic distributions in CoCrFeMnNi HEA-matrix.

2.2 Simulation procedure

The uniaxial tensile mechanical properties and reinforcement mechanism of CoCrFeMnNi high entropy alloy matrix laminated composites reinforced by the monolayer monolayer Ni-GNP-Ni are studied using molecular dynamics simulation software LAMMPS [11]. The atomic force fields in the Ni-GNP-Ni/CoCrFeMnNi models are defined by hybrid potential functions. The MEAM [12] potential is employed to represent the interactions between metal atoms; the covalent C–C bonding within the graphene layer is predicted by the AIREBO [13] potential; the Lennard-Jones (L-J) [14] potential function is employed to describe the van-der-Waals interactions between HEA atoms and C atoms in graphene, as well as between Ni and C atoms in Ni-GNP-Ni. Table 1 shows the L-J parameters. Prior to the tensile loading, the Conjugate Gradient (CG) method is applied to minimize the energy of Ni-Gr-Ni/CoCrFeMnNi systems. The systems are relaxed and equilibrated at 300 K under the NPT ensemble with a pressure of 0 bar by running 40,000 steps with a time step of 1 fs. During

uniaxial tensile simulation, the velocity-Verlet algorithm is used for the integral calculation of the classical Newton's moving equation. Periodic boundary conditions are applied in *x*, *y* and *z* directions to avoid the surface effect, while a constant strain rate of $1\times10^{9}s^{-1}$ is applied in the *y*-direction at 300 K. The structural evolution is characterized with the common neighbor analysis (CNA) and dislocation analysis (DXA) technique in OVITO [15].

Table 1: Parameters of Lennard-Jones (LJ) potential function [14]

Atom-pair	ε (eV)	σ (Å)
Co-C	0.038281	2.842
Cr-C	0.037758	2.868
Fe-C	0.038687	2.8605
Mn-C	0.038021	2.864
Ni-C	0.038429	2.841

3 RESULTS AND DISCUSSION

3.1 Ni‑GNP-Ni effect on tensile properties of CoCrFeMnNi and GNP/CoCrFeMnNi

The tensile stress‑strain curves of Ni-coated zigzag GNP and uncoated GNP-reinforced CoCrFeMnNi composites as well as monolithic CoCrFeMnNi at 300 K and 1×10^{9} s^{-1} are displayed in Fig. 2 for comparison. It can be seen that the stress‑strain curves for the above three materials have different characteristics although they all have gone through typical elastic, yielding, and plastic deformation stages. The Young's modulus can be determined by linear regression analysis for the elastic stage. Here, the Young's modulus for the Ni-GNP-Ni/HEA composites is about 110.52 GPa, while those for the GNP/HEA composites and the monolithic CoCrFeMnNi HEA are 109.25 and 101.44 GPa, respectively. It can be found that good agreement in elastic modulus(110.52GPa), peak stress (9.17GPa) and fracture strain (0.094) of single-crystal CoCrFeMnNi HEA between the present MD predictions and existing calculation results in reference [16] was achieved, preliminarily validating the applicability of our MD model. The enhancement in the elastic modulus of the Ni-GNP-Ni/ HEA composites is directly correlated with the improved interface bonding of the Ni-GNP-Ni to the HEA matrix and the reinforcing effect of graphene.

In addition, there is also a significant difference for the stress‑strain curves after the stress reaches the highest point (peak stress). For the Ni-GNP-Ni/HEA, the GNP/HEA composites, and the monolithic CoCrFeMnNi HEA, there all exist an ever-decreasing stage of the stress due to the nucleation of defects and a stress flow stage because of the interaction of defects after the stress reaches the peak stress, but a second large stress decrease stage occurs in the stress‑strain curves for the first two due to the GNP fracture (fracture stress) and the fracture propagation. Compared with the uncoated GNP/HEA composite and the monolithic CoCrFeMnNi matrix, the peak stress for the Ni-GNP-Ni/HEA composite is, respectively, increased by 15.27 and 20.17%, while its fracture stress is separately increased by 23.45 and

15.38%, showing that the Ni-GNP-Ni also contributes significantly to the strength of the uncoated GNP/HEA composite and the CoCrFeMnNi matrix.

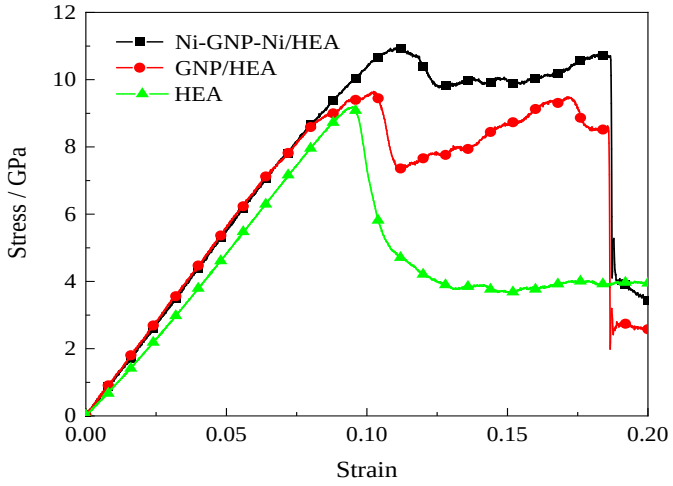

Figure 2: Stress-strain curves for uncoated and Ni coated GNP/CoCrFeMnNi HEA as well as monolithic CoCrFeMnNi HEA at 300 K and 1 $\times 10^9$ s^{-1}.

3.2 Temperature and strain‑rate effect on Ni-GNP-Ni/CoCrFeMnNi

The temperature effect on tensile properties of Ni-GNP-Ni/HEA composites at a strain rate of 1 $\times 10^9$ s^{-1} has been investigated and the results are shown in Fig. 3(a). It can be seen from Fig. 3(a) that the tensile properties of Ni-GNP-Ni/HEA composite have a strong temperature dependence. When the temperature is increased from 100 to 500 K, the oscillations in simulated stress-strain curves for the Ni-GNP-Ni/HEA composite become larger and more irregular; however, the elastic modulus, the peak stress and the corresponding strain, and the fracture stress and fracture strain of the Ni-GNP-Ni/HEA composite all appear to decrease. The Ni-GNP-Ni/HEA composite has an obvious temperature-softening effect. This is because the higher the temperature, the stronger the vibration and diffusion motion of atoms in the composite, resulting in the easier slip systems activation and more accelerated nucleation rate of pores.

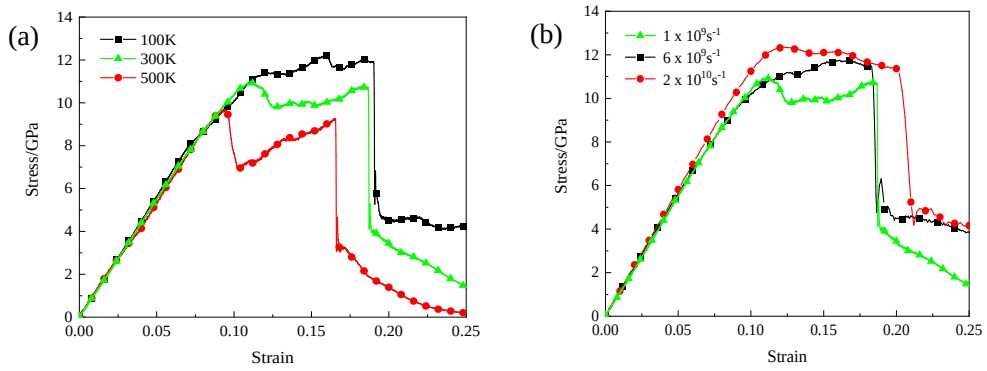

Figure 3: Tensile stress-strain curves of Ni-GNP-Ni/CoCrFeMnNi composites at (a) different temperatures and (b) different strain rates

Figure 3(b) depicts the tensile stress – strain curves of Ni-GNP-Ni/CoCrFeMnNi composites at 300 K and three typical strain rates, in which the longitudinal coordinates represent the average stress value of the Ni-GNP-Ni/CoCrFeMnNi composites in the *y* (tensile) direction. It can be seen from Fig. 3(b) that the stress-strain curves for the Ni-GNP-Ni/CoCrFeMnNi composites at different strain rates are almost coincident in the initial linear elastic stage during their tensile loading, indicating no obvious change in Young's modulus of the composites with strain rate. However, it should be noted that the peak stress, fracture stress and strain of the composites all increase with the increase of strain rate at different strain rates. At the lower strain rate (1×10^9 s^{-1}), the fluctuations in the stress-strain curves become larger after the second stress drop due to the Ni- GNP-Ni fracture, while at the higher strain rate (2×10^{10} s^{-1}), the tensile stress decreases more slowly after it reaches the peak stress. The variation in the stress-strain response after the elastic stage may be related to the plastic deformation mechanism of the composites at different strain rates.

3.3 Strengthening mechanism of Ni-GNP-Ni/CoCrFeMnNi composites

In order to well understand the strengthening effect of the introduction of the Ni-coated graphene on the mechanical behavior of the Ni-GNP-Ni/CoCrFeMnNi composites, we have compared the atomic configurations and dislocation evolutions of single crystal HEA and Ni-GNP-Ni/HEA composites during tensile process. Fig. 4 gives the atomic configurations of the single crystal CoCrFeMnNi and Ni-GNP-Ni/CoCrFeMnNi composites subjected to tension loading at various strains. As shown in Fig. 6, although there existed HCP stacking faults in both the single crystal HEA and Ni-GNP-Ni/CoCrFeMnNi composites, the HCP stacking faults in the latter occurred on both sides of the interface and expand in the matrix almost simultaneously with a symmetrical distribution about the interface, while the expansion of stacking faults is hindered by Ni-GNP-Ni reinforcement. Moreover, multiple disordered atomic structures began to appear near the interface of the composites as the strain increases, and defects initiated from the interface expanded along the crystal planes inside the HEA matrix. The deformation and strength of the composites are mainly dominated by the interface, and Ni-coated graphene plays an effective role in load transfer.

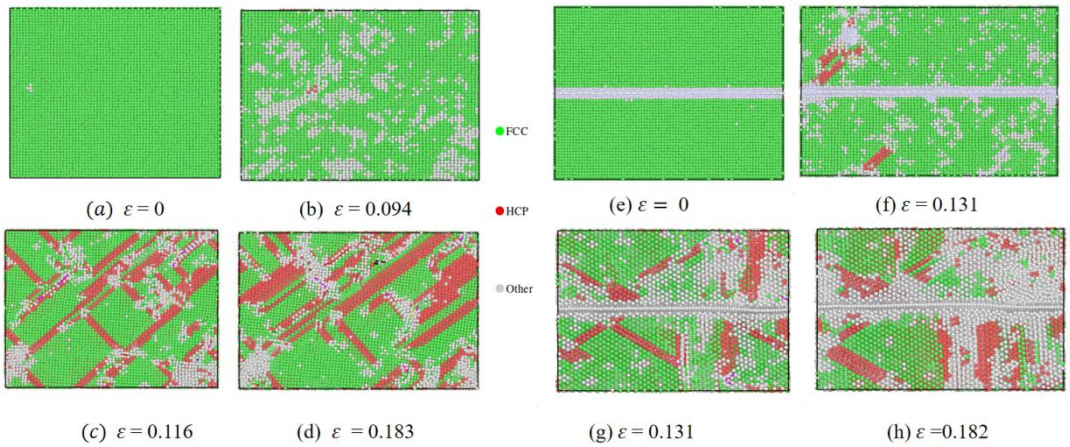

Figure 4: Atomic configurations of (a)-(d) single crystal CoCrFeMnNi and (e)-(h) Ni-GNP-Ni/CoCrFeMnNi composites under different tensile strains

Fig. 5 shows the distribution of dislocation lines of single-crystal CoCrFeMnNi HEA and the Ni-GNP-Ni/ CoCrFeMnNi composite under different strains. It can be seen from Fig. 5(a) that after entering the plastic stage, a lot of long dislocation lines appear in single-crystal CoCrFeMnNi HEA. And with the increase of strain, the rate of dislocation annihilation is the same as that of dislocation nucleation, and the density of dislocation remains unchanged, as shown in Fig. 5(a). Therefore, there is no plastic strain strengthening in single-crystal CoCrFeMnNi HEA. However, more and shorter dislocation lines are induced in the Ni-GNP-Ni/CoCrFeMnNi composites, as shown in Fig. 5(b). It can be found that the dislocation movement in the HEA matrix is strongly suppressed by the Ni-coated graphene. It is difficult for dislocations to cut across the Ni-coated graphene into the adjacent layer due to the high strength of graphene. As a result, the stress of the Ni-GNP-Ni/CoCrFeMnNi composites continues to increase with the increase of strain in the plastic deformation stage, as shown in Fig. 2. Moreover, with the strain increases, the increase of the dislocation density at the interface will strongly suppress or inhibit the motion of dislocations, and the strengthening effect is more obvious. In addition, the results show that in the later stage of plastic deformation, the stress of the Ni-GNP-Ni/CoCrFeMnNi composites suddenly decreases for the second time, which is due to the fracture of Ni-coated graphene.

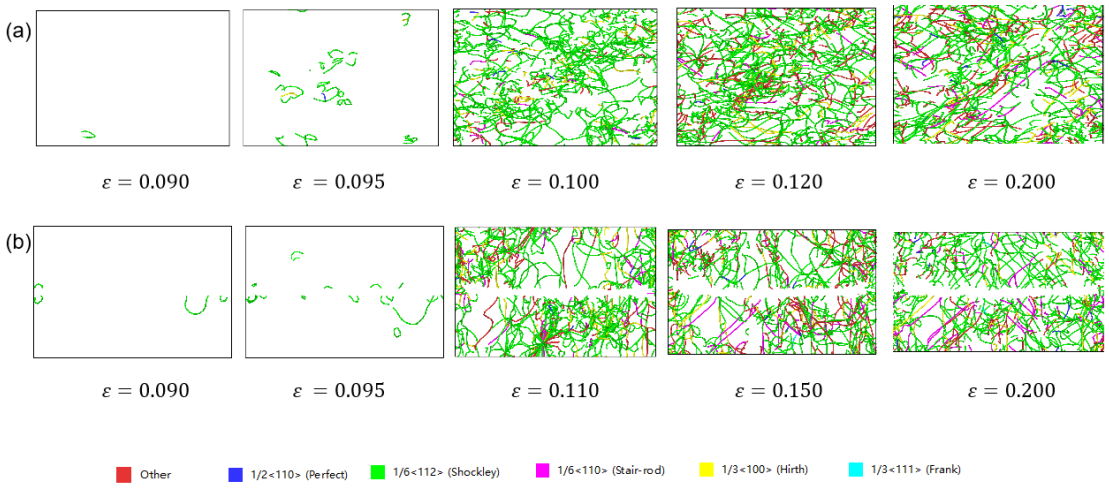

Figure 5: Distribution of dislocation lines in (a) single HEA and (b) Ni-GNP-Ni/CoCrFeMnNi composites under different strains.

4 CONCLUSIONS

- MD simulations of uniaxial tension of Ni-GNP-Ni/CoCrFeMnNi HEA matrix composites at different temperatures and strain rates have shown that the Ni-coated graphene can effectively enhance the elastic modulus and tensile strength of the composites.
- Temperature and strain rate have a strong influence on the tensile mechanical properties of Ni-GNP-Ni/CoCrFeMnNi composites. The mechanical properties of the laminated composites have strain hardening and temperature softening effects. The composites show good overall mechanical behavior at low temperature and high strain rate.

- For Ni-GNP-Ni/CoCrFeMnNi laminated composites, Interface strengthening, effective load transfer, and dislocation strengthening are the main reinforcement mechanisms.

REFERENCES

[1] Gludovatz, B. Hohenwarter, A. Catoor, D. Chang, E.H, George, E.P. and Ritchie, R.O. A fracture-resistant high-entropy alloy for cryogenic applications. *Science* (2014) **345**: 1153-1158.

[2] An, Z. Mao, S. Liu, Y, Zhou, H. Zhai, Y. Tian, Z. Liu, C. and Zhang, Z. Hierarchical grain size and nanotwin gradient microstructure for improved mechanical properties of a non-equiatomic CoCrFeMnNi high-entropy alloy. *J. Mater. Sci. Technol.* (2021) **92**: 195-207.

[3] Lian, G. Yang, J. Que, L. Lan, R. and Tang, X. Effect of Ti content on the microstructure and properties of $CoCrFeNiMnTi_x$ high entropy alloy prepared by laser cladding. *J. Mater. Sci.* (2024) **59**:1027–1043.

[4] Guo, W. Li, J. Qi, M. Xu, Y. Ezatpour, H.R. Mechanical performances and processing-property modeling for Al0.3CoCrFeNiMn high-entropy alloy. *J. Alloy. Compd.* (2022) **905**: 163791.

[5] Tian, Y.Z. Peng, S.Y. Chen, S. F. Gu, Z.J. Yang, Y. Shang, X.L. Deng, G.Y. Su, L. H. and Sun, S.J. Temperature-dependent tensile properties of ultrafine-grained C-doped CoCrFeMnNi high-entropy alloy. *Rare Met.* (2022) **41**: 2877-2885.

[6] Son, S. Lee, J. Asghari-Rad, P. Gu, G.H. Haftlang, F. and Kim, H.S. A facile strengthening method by co-doping boron and nitrogen in CoCrFeMnNi high-entropy alloy. *Mat. Sci. Eng. A-Struct.* (2022) **846**: 143307.

[7] Liu, C. Jiang, X. Sun, H. Zhang, Y. Fang, Y. and Shu, R. Microstructure and mechanical properties of bioinspired laminated CoCrFeNiMn high entropy alloy matrix composites reinforced with graphene. *Mat. Sci. Eng. A-Struct.* (2022) **859**: 144198.

[8] Grazianetti, C. and Molle, A. Engineering epitaxial silicene onfunctional substrates for nanotechnology. *Research* (2019) **2019**: 8494606.

[9] Lata, P. Singh, D. Pandel, U. and Duchaniya. R.K. Graphene oxide reinforced high entropy alloy (CuNiFeCrMo-GO) nanocomposite coating deposited by electroless coating method on mild steel. *Mater. Today: Proc.* (2020) **28**: 2411-2417.

[10] Liu, C. Jiang, X. Sun, H.Liu, T. Wu, Z. and Yang, L. Preparation of graphene film reinforced CoCrFeNiMn high-entropy alloy matrix composites with strength-plasticity synergy via flake powder metallurgy method. *J. Mater. Res. Technol.* (2023) **27**: 7614-7626.

[11] Thompson, A.P. Aktulga, H.M. Berger, B. Bolintineanu, D.S. Brown, W.M. Crozier, P.S. et al. LAMMPS-a flexible simulation tool for particle-based materials modeling at the atomic, meso, and continuum scales. *Comput. Phys. Commun.* (2022) **271**: 108171.

[12] Choi, W.M. Jo, Y.H. Sohn, S.S. and Lee, B.J. Understanding the physical metallurgy of the CoCrFeMnNi high-entropy alloy: an atomistic simulation study. *Npj Comput. Mater.* (2018) **4**: 1-9.

[13] Stuart, S.J. Tutein, A.B. Judith, A. and Harrison, J.A. A reactive potential for

hydrocarbons with intermolecular interactions. *J. Chem. Phys.* (2000) **112**: 6472-6486.
[14] Tang, Y. and Li, D.Y. Nano-tribological behavior of high-entropy alloys CrMnFeCoNi and CrFeCoNi under different conditions: A molecular dynamics study. *Wear* (2021) **476**: 203583.
[15] Stukowski, A. Visualization and analysis of atomistic simulation data with OVITO–the Open Visualization Tool. *Modelling Simul. Mater. Sci. Eng.* (2010) **18**: 015012.
[16] Zhang, Z. Kou, J. Chen, L. Guo, J. Duan, X.Y. Shan, B. and Duan, X. From stacking fault to phase transformation: A quantitative model of plastic deformation of CoCrFeMnNi under different strain rates. *Intermetallics* (2022) **146**: 107585.